



CONVECTION-DIFFUSION OF SOLUTES IN MEDIA WITH PIECEWISE CONSTANT TRANSPORT PROPERTIES

DURGESH S. VAIDYA, J. M. NITSCHKE, S. L. DIAMOND and DAVID A. KOFKE

Department of Chemical Engineering, State University of New York at Buffalo, Buffalo, NY 14260-4200,
U.S.A.

(First received 13 July 1995; revised manuscript received and accepted 16 April 1996)

Abstract—Motivated by applications to electrophoretic techniques for bioseparations, we consider transverse one-dimensional convection–diffusion through a medium in which the solute diffusivity and convective velocity undergo step changes at a prescribed position. An exact method of solution of the governing transport equations is formulated in terms of a largely analytical approach representing a novel alternative to the self-adjoint formalism advanced by Ramkrishna and Amundson (1974, *Chem. Engng Sci.* **29**, 1457–1464), and applied recently by Locke and Arce (1993, *Chem. Engng Sci.* **48**, 1675–1686) and Locke *et al.* (1993, *Chem. Engng Sci.* **48**, 4007–4022). A concentration boundary layer of $O(Pe^{-1})$ thickness is found to form at the upstream side of the interface. No concentration boundary layer exists on the downstream side. The exact solution is supplemented with an asymptotic analysis for large Péclet numbers, Pe . Detailed study of the boundary layer reveals interesting features of the local dynamical processes whereby the interface—infinitesimally thin macroscopically—appears as an effective source or sink of the solute content. The asymptotic analysis has direct utility in accurate prediction of concentration profiles for high Péclet number operations where analytical approaches break down and finite-difference methods require tremendous computational time to achieve sufficient accuracy and resolution. Copyright © 1996 Elsevier Science Ltd

Keywords: Convection–diffusion, boundary layer, interface.

1. INTRODUCTION

Mass transport through a medium with discontinuous variations in physical properties is of interest in the study of composite materials, as well as membranes, gels and liquid–liquid interfaces. Such a study finds applications in purification and separation methods for organic compounds and biological molecules. Ramkrishna and Amundson (1974) proposed the self-adjoint formulation for modeling convection–diffusion through a stationary composite medium. This method was extended by Locke and Arce (1993) and Locke *et al.* (1993) to include reaction within each slab of the composite material [also see Arce and Locke (1994)]. Hladky (1987) studied steady-state diffusion and convection of solutes (tritiated water, methanol, ethanol, and *n*-propanol) across a water–octanol interface. Bulk solvent convection was assumed to be negligible near the interface and the thickness of the ‘unstirred layer’ was estimated from experimental data. Levine and Bier (1990) and Clark (1992) have experimentally investigated the electromigration and partitioning of proteins across a two-phase aqueous interface. Numerical results using finite-difference (FD) techniques for this system were given by Levine *et al.* (1992). More recently (Raj, 1994), with the development of counteracting chromatographic electrophoresis (CACE), the features of gel permeation chromatography and gel electrophoresis were combined to purify and separate a target protein

at the junction of two gels. In CACE, the entire separation takes place at the interface; the rest of the gel length does not contribute toward separation. In spite of the extent of experimental and numerical results for transport across interfaces, a fundamental understanding of the dynamics of solute transport in the region near the interface (the boundary layer) has yet to be fully developed, especially at large Péclet numbers.

In the present study, the convection–diffusion equation describing transport through a surface across which material properties change is investigated via two complementary methods for the case where there is no reaction within the bulk of the medium. Moreover, we have assumed that partitioning across the interface occurs via rapid local equilibrium. Section 2 presents the governing equations along with the initial and boundary conditions. In Section 3, we develop a largely analytical solution method different from but comparable to the method of Locke and Arce (1993) and Locke *et al.* (1993). (The details of comparison between the two methods are mentioned after eq. (39) below.) In Section 4, we develop a perturbation analysis for large Péclet numbers motivated by the fact that diffusion is dominated by convection in liquid electrophoresis and electropartitioning, to such an extent that typically $Pe = O(10^5)$. This large value represents a regime inaccessible to calculations by analytical means. Detailed study of the asymptotic

behavior in the regime of large Pe greatly simplifies the computational effort for evaluating the concentration evolution across an interface due to reduction of the full-fledged second-order PDE into a sequence of first-order PDEs. The inner and outer solutions for the solute concentration profile reveal the dynamical processes operative in a thin boundary layer near the interface and their consequences for transport throughout the medium. Specifically, it reveals new boundary conditions (jump conditions) that need to be imposed on the outer (macroscopic) solutions in order to satisfy requirements of rapid equilibrium and continuity of flux across the interface. We emphasize that by an interface we mean a singular surface across which transport properties of a solute undergo a sudden change but that the surface itself offers no mass transfer resistance to the solute.

In addition to static interfaces, there have been several attempts to make the two-phase boundary dynamic. Grimshaw *et al.* (1989) have fabricated membranes with properties that can be chemically and electrically modulated over a period of time. Ly and Cheng (1993) have designed liquid crystalline membranes with an electrically controlled permeability. With liquid crystals gaining increasing applications in chemical engineering, it is conceivable that the location of the interface can also be modulated in a time-dependent manner. With this in mind, the large Péclet number analysis has been extended to dynamic media with arbitrary user-imposed interface velocities in Appendix B.

2. FORMULATION

Consider transient, one-dimensional convective-diffusive transport of a solute in a dilute solution where the convective velocity, v , and the diffusivity, D , are uniform except for a discontinuity at a plane surface at position $x = L_f$ (Fig. 1). Throughout this paper, we will use superscript $i = I$ to distinguish the left (upstream) region ($0 \leq x \leq L_f$) and $i = II$ for the right-hand side (downstream) domain ($L_f \leq x \leq L$). For such a discontinuous medium, the conservation equation can be represented as

$$\frac{\partial c^i}{\partial t} = D^i \frac{\partial^2 c^i}{\partial x^2} - v^i \frac{\partial c^i}{\partial x}, \quad i = I, II. \quad (1)$$

The solute's convective velocity v^i represents a superposition of fluid flow and electrophoretic migration in an applied field. Any fluid flow contribution is neces-

sarily constant by mass conservation in one dimension. The speed of electrophoretic migration relative to the fluid generally depends upon the gel microstructure, and so differs between regions I and II; this is the contribution that imparts a discontinuity to the solute velocity. At low solute concentrations, i.e. when the solute does not contribute significantly to the conductivity of the medium, the electrophoretic migration velocity is simply the product of the electric field, E , and a mobility equal to zFD^i/RT where z is the valency of the solute, F is Faraday's constant, R is the universal gas constant, and T is temperature.

We will consider two modes of operation of the column.

2.1. Problem 1: no flux at entrance

For this problem, we assume that at time $t = 0$ the column contains a prescribed initial distribution of the solute. At all positive times, there is no solute flux entering the column from upstream. The section of the column beyond $x = L$ is both infinite in length and well-mixed, so that Danckwerts' boundary conditions hold (Danckwerts, 1953; Novy *et al.*, 1990). Therefore,

$$c^i(x, 0) = f^i(x), \quad i = I, II \quad (2)$$

$$-D^I \frac{\partial c^I(0, t)}{\partial x} + v^I c^I(0, t) = 0, \quad t > 0 \quad (3)$$

$$\frac{\partial c^{II}(L, t)}{\partial x} = 0, \quad t > 0. \quad (4)$$

2.2. Problem 2: constant flux at entrance

In this case, at time $t = 0$ the column is empty. For all later times, there is a constant input concentration c_{inp} flowing into the column. The initial condition along with the boundary conditions are

$$c^i(x, 0) = 0, \quad i = I, II \quad (5)$$

$$-D^I \frac{\partial c^I(0, t)}{\partial x} + v^I c^I(0, t) = v^I c_{inp}, \quad t > 0 \quad (6)$$

$$\frac{\partial c^{II}(L, t)}{\partial x} = 0, \quad t > 0. \quad (7)$$

For both problems, the concentrations on either side of the interface are related to each other via the requirements of local equilibrium and continuity of flux, leading to the matching conditions:

$$c^I(L_f, t) = K_{eq} c^{II}(L_f, t), \quad t > 0 \quad (8)$$

$$-D^I \frac{\partial c^I(L_f, t)}{\partial x} + v^I c^I(L_f, t)$$

$$= -D^{II} \frac{\partial c^{II}(L_f, t)}{\partial x} + v^{II} c^{II}(L_f, t), \quad t > 0. \quad (9)$$

The jump in velocity and diffusivity across the interface is due to a change in the tortuosity of the medium while the equilibrium constant K_{eq} of the solute is dictated by the change in the porosity of the medium.

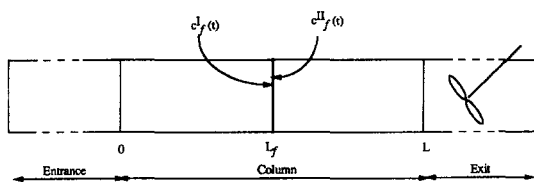


Fig. 1. Column containing discontinuous medium with the interface located a distance L_f from the entrance.

Equations (1)–(9) determine the time evolution of the solute concentration throughout the column. Our goal in the following sections is to devise two approaches to the solution of these equations for $c^i(x, t)$.

3. ANALYTICAL SOLUTION

Considerable progress can be made using pencil and paper with eqs (1)–(9) and we shall proceed analytically as far as possible in order to gain theoretical understanding and reduce the computational effort.

Two key quantities in our solution are the time-dependent values of the left- and right-hand side solute concentrations at the interface ($x = L_f$); we shall denote these by $c_f^I(t)$ and $c_f^{II}(t)$, respectively. They are not known *a priori* but will be determined subsequently. Thus, we write

$$c^I(L_f, t) \equiv c_f^I(t), \quad t > 0 \tag{10}$$

$$c^{II}(L_f, t) \equiv c_f^{II}(t), \quad t > 0. \tag{11}$$

Our approach is to temporarily regard $c_f^I(t)$ and $c_f^{II}(t)$ as known, and to solve for the concentration distributions $c^I(x, t)$ and $c^{II}(x, t)$ in terms of these two time-dependent functions. Only subsequently do we impose the matching conditions (8) and (9), which then determine $c_f^I(t)$ and $c_f^{II}(t)$, thereby completing the solution for the concentration distribution.

We define new dependent variables $s^I(x, t)$ and $s^{II}(x, t)$, in lieu of $c^I(x, t)$ and $c^{II}(x, t)$, such that boundary conditions in each domain become homogeneous and the convective term in eq. (1) is eliminated. These simplifications are achieved by making the transformations

$$c^I(x, t) = s^I(x, t) \exp \left[\frac{v^I}{2D^I} (x - L_f) - \frac{(v^I)^2}{4D^I} t \right] + c_f^I(t) \exp \left[\frac{v^I}{D^I} (x - L_f) \right] \tag{12}$$

$$c^{II}(x, t) = s^{II}(x, t) \exp \left[\frac{v^{II}}{2D^{II}} (x - L_f) - \frac{(v^{II})^2}{4D^{II}} t \right] + c_f^{II}(t). \tag{13}$$

For problem 1, the modified concentration variables $s^I(x, t)$ and $s^{II}(x, t)$ are then governed by the respective initial and boundary value problems listed below:

$$\begin{aligned} 0 \leq x \leq L_f & & L_f \leq x \leq L \\ \frac{\partial s^I}{\partial t} - D^I \frac{\partial^2 s^I}{\partial x^2} & & \frac{\partial s^{II}}{\partial t} - D^{II} \frac{\partial^2 s^{II}}{\partial x^2} \\ = W^I(t) P^I(x) & & = W^{II}(t) P^{II}(x) \end{aligned} \tag{14}$$

$$s^I(x, 0) = g^I(x) \quad s^{II}(x, 0) = g^{II}(x) \tag{15}$$

$$\frac{\partial s^I(0, t)}{\partial x} + h^I s^I(0, t) = 0 \quad \frac{\partial s^{II}(L, t)}{\partial x} + h^{II} s^{II}(L, t) = 0 \tag{16}$$

$$s^I(L_f, t) = 0 \quad s^{II}(L_f, t) = 0, \tag{17}$$

where

$$W^i(t) = - \frac{dc_f^i}{dt} \exp(a^i t) \tag{18}$$

$$P^i(x) = \exp[h^i (x - L_f)] \tag{19}$$

$$g^I(x) = \{ f^I(x) \exp[-h^I (x - L_f)] - \{ c_f^I(0) \exp[h^I (x - L_f)] \} \} \tag{20}$$

$$g^{II}(x) = \{ f^{II}(x) - c_f^{II}(0) \} \exp[-h^{II} (x - L_f)] \tag{21}$$

and we have used the symbols h^i and a^i to denote $(v^i/2D^i)$ and $(v^i)^2/4D^i$, respectively, with $i = I$ or II .

Applying the method of separation of variables (Weinberger, 1965a), the discrete spectrum of eigenvalues α_n^i of the Sturm–Liouville problem (Weinberger, 1965b) associated with eqs (14)–(17) is given by

$$h^I \sin(\alpha_n^I L_f) + \alpha_n^I \cos(\alpha_n^I L_f) = 0 \tag{22}$$

$$h^{II} \sin[\alpha_n^{II} (L - L_f)] + \alpha_n^{II} \cos[\alpha_n^{II} (L - L_f)] = 0, \quad n = 1, 2, 3 \dots \tag{23}$$

The corresponding orthogonal and complete basis functions (Weinberger, 1965b; Kreyszig, 1993) take the form

$$X_n^i(x) = \sin[\alpha_n^i (x - L_f)], \quad n = 1, 2, 3 \dots \tag{24}$$

The concentration profile $s^i(x, t)$ can then be written as

$$s^i(x, t) = \sum_{n=1}^{\infty} A_n^i(t) X_n^i(x) \tag{25}$$

where $A_n^i(t)$ are time-dependent Fourier coefficients. The right-hand-side functions $P^i(x)$ given by eq. (19) can be expanded in terms of the basis functions as follows:

$$P^i(x) = \sum_{n=1}^{\infty} p_n^i X_n^i(x) \tag{26}$$

where the Fourier coefficients of $P^i(x)$ are given by

$$p_n^i = \frac{\int P^i(x) X_n^i(x) dx}{\int [X_n^i(x)]^2 dx} \tag{27}$$

The interval of integration is $[0, L_f]$ and $[L_f, L]$, respectively, for $i = I$ or II .

The expressions for $s^i(x, t)$ in eq. (25), $W^i(t)$ in eq. (18), and $P^i(x)$ given by eq. (26) are substituted in eq. (14). Solving the resultant ODE term by term in n , we obtain the expression for the time-dependent Fourier coefficients $A_n^i(t)$ as

$$A_n^i(t) = \exp[-(\alpha_n^i)^2 D^i t] \left\{ A_n^i(0) + p_n^i \int_0^t - \frac{dc_f^i}{d\tau} \times \exp(a^i \tau) \exp[(\alpha_n^i)^2 D^i \tau] d\tau \right\} \tag{28}$$

In eq. (28), $A_n^i(0)$ denotes the value of $A_n^i(t)$ at time $t = 0$. In order to satisfy the initial condition (15) for the modified concentration profile of the form given by eq. (25), the coefficients $A_n^i(0)$ have to equal the

Fourier coefficients of the modified initial distributions $g^i(x)$ for $i = I, II$, respectively. Therefore,

$$A_n^i(0) = \frac{\int g^i(x) X_n^i(x) dx}{\int [X_n^i(x)]^2 dx} \tag{29}$$

Once again, the interval of integration is $[0, L_f]$ and $[L_f, L]$, respectively, for $i = I$ or II . The integral (27) can be evaluated explicitly:

$$p_n^I = \frac{-4(\alpha_n^I)^2}{[(\alpha_n^I)^2 + (h^I)^2] [(2\alpha_n^I L_f) - \sin(2\alpha_n^I L_f)]} \tag{30}$$

$$p_n^{II} = \frac{4(\alpha_n^{II})^2}{[(\alpha_n^{II})^2 + (h^{II})^2] \{ [2\alpha_n^{II}(L - L_f)] - \sin [2\alpha_n^{II}(L - L_f)] \}} \tag{31}$$

At this stage, the only unknowns in the determination of $s^I(x, t)$ and $s^{II}(x, t)$ are the interfacial concentration distributions $c_f^I(t)$ and $c_f^{II}(t)$. Substitution of the preceding representation eq. (25) of $s^I(x, t)$ and $s^{II}(x, t)$ into eqs (12) and (13) and subsequent substitution of the form of $c^i(x, t)$ into the interface conditions of eqs (8) and (9) leads, after considerable algebra, to the following integrodifferential equation for $c_f^i(t)$:

$$Q(t) + K_{eq} \int_0^t \frac{dc_f^i}{d\tau} G^i(t; \tau) d\tau = \int_0^t \frac{dc_f^i}{d\tau} G^{ii}(t; \tau) d\tau + v^{ii} c_f^i(t) \tag{32}$$

where

$$b_n^I = (\alpha_n^I)^2 D^I \tag{33}$$

$$b_n^{II} = (\alpha_n^{II})^2 D^{II} \tag{34}$$

$$Q^I(t) = -D^I \exp(-a^I t) \sum_{n=1}^{\infty} A_n^I(0) \alpha_n^I \exp(-b_n^I t) \tag{35}$$

$$Q^{II}(t) = -D^{II} \exp(-a^{II} t) \sum_{n=1}^{\infty} A_n^{II}(0) \alpha_n^{II} \exp(-b_n^{II} t) \tag{36}$$

$$G^I(t; \tau) = D^I \exp[-a^I(t - \tau)] \times \sum_{n=1}^{\infty} \alpha_n^I p_n^I \exp[-b_n^I(t - \tau)] \tag{37}$$

$$G^{II}(t; \tau) = D^{II} \exp[-a^{II}(t - \tau)] \times \sum_{n=1}^{\infty} \alpha_n^{II} p_n^{II} \exp[-b_n^{II}(t - \tau)] \tag{38}$$

$$Q(t) = Q^I(t) - Q^{II}(t). \tag{39}$$

Solution of eq. (32) gives the evolution of the interfacial concentration on the downstream side. That on the upstream side is quickly evaluated via the condition of local equilibrium viz., eq. (8). These interfacial concentrations can be substituted in eq. (28) to obtain

the time-dependent Fourier coefficients of the distributions $s^i(x, t)$. The concentration profiles are then obtained via eqs (12), (13) and (25). Computational details have been outlined in Appendix A.

It is worthwhile to compare briefly the present approach with that of Locke and Arce (1993) and Locke *et al.* (1993). These authors determine a sequence of eigenvalues λ_n^i applicable to the whole M -layer (here two-layer) domain $0 < x < L$, for which the corresponding eigenfunctions $u_n(x)$ are given by a set of M formulas (each formula applying to one of the layers). The solution of the transport problem is then given as a single Fourier series in the $u_n(x)$ in which the Fourier coefficients contain the factors $\exp(-\lambda_n^i t)$. The present approach develops a sequence of eigenvalues and eigenfunctions, and a corresponding spectral expansion, for each layer. These separate expansions are then pieced together in a manner that focuses on the time dependence of the interfacial concentration $c_f^i(t)$, which is found to be governed by an integrodifferential equation. Reformulation of a differential equation in terms of an integral equation of lower dimensionality is quite common for both theoretical and numerical purposes. Thus, for instance, this general approach is used in the theory of ODE [e.g. Ince (1956)], and it forms the basis of boundary integral methods in Stokes fluid mechanics [e.g. Kim and Karrila (1991)].

Problem 2 can be solved in the same manner as problem 1 if one now defines (Brenner, 1962) $\rho^I(x, t) = c^I(x, t) - c_{inp}$. For convenience of notation, we may trivially define $\rho^{II}(x, t) = c^{II}(x, t)$. In addition, we denote $\rho_f^I \equiv \rho^I(L_f, t)$, and $\rho_f^{II} \equiv \rho^{II}(L_f, t)$. The initial and boundary conditions now take the familiar form

$$\rho^I(x, 0) = -c_{inp} \tag{40}$$

$$\rho^{II}(x, 0) = 0 \tag{41}$$

$$-D^I \frac{\partial \rho^I(0, t)}{\partial x} + v^I \rho^I(0, t) = 0, \quad t > 0 \tag{42}$$

$$\frac{\partial \rho^{II}(L, t)}{\partial x} = 0, \quad t > 0. \tag{43}$$

The solution for ρ^i proceeds in the same manner as that for c^i in problem 1 except for two modifications. Equations (8) and (9) are replaced by

$$\rho_f^I(t) + c_{inp} = K_{eq} \rho_f^{II}(t) \tag{44}$$

$$-D^I \frac{\partial \rho^I(L_f, t)}{\partial x} + v^I \rho^I(L_f, t) + v^I c_{inp} = -D^{II} \frac{\partial \rho^{II}(L_f, t)}{\partial x} + v^{II} \rho^{II}(L_f, t). \tag{45}$$

Finally, eq. (32) is modified as follows:

$$Q(t) + v^I c_{inp} + K_{eq} \int_0^t \frac{d\rho_f^{II}}{d\tau} G^I(t; \tau) d\tau = \int_0^t \frac{d\rho_f^I}{d\tau} G^{II}(t; \tau) d\tau + v^{II} \rho_f^{II}(t). \tag{46}$$

The actual concentration profile in each domain is then recovered by realizing that $c^I(x, t) = \rho^I(x, t) + c_{\text{inp}}^I$ [and trivially, $c^{II}(x, t) = \rho^{II}(x, t)$].

4. PERTURBATION ANALYSIS FOR LARGE PÉCLET NUMBER

The case of large Péclet number $Pe = \bar{v}L/\bar{D}$; see eq. (55) below] frequently arises in real applications, particularly in transport phenomena occurring in un-packed columns. For example, in liquid electrophoresis, the convective velocity of a solute, in the absence of electro-osmotic flow, is coupled to its molecular diffusivity via the mobility constant. For this application, $v^i \sim O(10^{-4})$ m/s, $D^i \sim O(10^{-9})$ m²/s, $L \sim O(1)$ m and hence $Pe \sim O(10^5)$. For accurate determination of the concentration profile near the interface, finite-difference techniques require extremely fine meshes of around 2000 nodes per length of column. Stability of such schemes demands also very small time steps; thus, to obtain useful results one requires extremely large computation times. By performing a perturbation analysis for large Péclet numbers, we obtain a detailed understanding of the fine structure of the concentration profile near the interface seen in the numerical solution while simultaneously gaining considerable savings in computation time.

To begin with we define the small parameter $\epsilon = 1/Pe$ and cast eqs (1)–(4) in terms of dimensionless variables as follows:

$$\frac{\partial c^i}{\partial \tau} = \epsilon \phi^i \frac{\partial^2 c^i}{\partial \xi^2} - \mu^i \frac{\partial c^i}{\partial \xi} \tag{47}$$

$$c^i(\xi, 0) = f^i(\xi) \tag{48}$$

$$-\epsilon \phi^I \frac{\partial c^I(0, \tau)}{\partial \xi} + \mu^I c^I(0, \tau) = 0 \tag{49}$$

$$\frac{\partial c^{II}(1, \tau)}{\partial \xi} = 0. \tag{50}$$

At the interface, $\xi_f = L_f/L$, eqs (8) and (9) can be written in an equivalent form as

$$c^I = K_{\text{eq}} c^{II} \tag{51}$$

$$-\epsilon \phi^I \frac{\partial c^I}{\partial \xi} + \mu^I c^I = -\epsilon \phi^{II} \frac{\partial c^{II}}{\partial \xi} + \mu^{II} c^{II}. \tag{52}$$

Here the variables have been defined as

$$\bar{D} = \frac{D^I + D^{II}}{2}, \quad \bar{v} = \frac{v^I + v^{II}}{2} \tag{53}$$

$$\tau = \frac{t\bar{v}}{L}, \quad \xi = \frac{x}{L} \tag{54}$$

$$Pe = \frac{\bar{v}L}{\bar{D}}, \quad \epsilon = \frac{1}{Pe} \tag{55}$$

$$\phi^i = \frac{D^i}{\bar{D}}, \quad \mu^i = \frac{v^i}{\bar{v}}. \tag{56}$$

4.1. Outer region

For large Pe , diffusional effects are negligible away from the interface. Hence, in the outer region the solution may be expanded in a regular perturbation series

$$c^{i,\text{out}}(\xi, \tau) = c_0^{i,\text{out}}(\xi, \tau) + \epsilon c_1^{i,\text{out}}(\xi, \tau) + \epsilon^2 c_2^{i,\text{out}}(\xi, \tau) + \dots \tag{57}$$

We may express the given arbitrary initial distribution as

$$f^i(\xi) = f_0^i(\xi) + \epsilon f_1^i(\xi) + \epsilon^2 f_2^i(\xi) + \dots \tag{58}$$

Comparing zeroth- and first-order terms we obtain the successive governing first-order differential equations

$$\frac{\partial c_0^{i,\text{out}}}{\partial \tau} + \mu^i \frac{\partial c_0^{i,\text{out}}}{\partial \xi} = 0 \tag{59}$$

$$\frac{\partial c_1^{i,\text{out}}}{\partial \tau} + \mu^i \frac{\partial c_1^{i,\text{out}}}{\partial \xi} = \phi^i \frac{\partial^2 c_0^{i,\text{out}}}{\partial \xi^2} \tag{60}$$

subject to the auxiliary conditions

$$c_0^{i,\text{out}}(\xi, 0) = f_0^i(\xi) \tag{61}$$

$$c_1^{i,\text{out}}(\xi, 0) = f_1^i(\xi). \tag{62}$$

4.2. Inner region

In the region near the interface, concentration changes are expected to occur over distances of order ϵ . To resolve this boundary layer structure, we introduce the stretched coordinate $\zeta = (\xi - \xi_f)/\epsilon$, in terms of which eq. (47) becomes

$$\epsilon \frac{\partial c^i}{\partial \tau} = \phi^i \frac{\partial^2 c^i}{\partial \zeta^2} - \mu^i \frac{\partial c^i}{\partial \zeta}. \tag{63}$$

Proceeding again with a regular perturbation expansion, the inner solution takes the form

$$c^{i,\text{in}}(\zeta, \tau) = c_0^{i,\text{in}}(\zeta, \tau) + \epsilon c_1^{i,\text{in}}(\zeta, \tau) + \epsilon^2 c_2^{i,\text{in}}(\zeta, \tau) + \dots \tag{64}$$

Collecting terms of order ϵ^0 and ϵ^1 , we obtain the differential equations:

$$\phi^i \frac{\partial^2 c_0^{i,\text{in}}}{\partial \zeta^2} - \mu^i \frac{\partial c_0^{i,\text{in}}}{\partial \zeta} = 0 \tag{65}$$

$$\phi^i \frac{\partial^2 c_1^{i,\text{in}}}{\partial \zeta^2} - \mu^i \frac{\partial c_1^{i,\text{in}}}{\partial \zeta} = \frac{\partial c_0^{i,\text{in}}}{\partial \tau} \tag{66}$$

which apply both to the left and right regions of the interface ($\zeta < 0$ and $\zeta > 0$, respectively). The successive differential equations are supplemented with auxiliary conditions of fast equilibrium and continuity of flux expressed by eqs (8) and (9). Thus, by equating terms of like power in ϵ , we find

$$c_0^{i,\text{in}} = K_{\text{eq}} c_0^{II,\text{in}} \tag{67}$$

$$c_1^{i,\text{in}} = K_{\text{eq}} c_1^{II,\text{in}} \tag{68}$$

and at the interface $\zeta = 0$:

$$-\phi^I \frac{\partial c_0^{I,\text{in}}}{\partial \zeta} + \mu^I c_0^{I,\text{in}} = -\phi^{II} \frac{\partial c_0^{II,\text{in}}}{\partial \zeta} + \mu^{II} c_0^{II,\text{in}} \quad (69)$$

$$-\phi^I \frac{\partial c_1^{I,\text{in}}}{\partial \zeta} + \mu^I c_1^{I,\text{in}} = -\phi^{II} \frac{\partial c_1^{II,\text{in}}}{\partial \zeta} + \mu^{II} c_1^{II,\text{in}}. \quad (70)$$

The general solution of the preceding equations, subject to the requirements of at most algebraic divergence as $\zeta \rightarrow \pm \infty$ is

$$c_0^{I,\text{in}}(\zeta, \tau) = r^I(\tau) \left[1 + \left(K_{\text{eq}} \frac{\mu^I}{\mu^{II}} - 1 \right) \exp(v^I \zeta) \right] \quad (71)$$

$$c_0^{II,\text{in}}(\zeta, \tau) = r^{II}(\tau) \quad (72)$$

$$\begin{aligned} c_1^{I,\text{in}}(\zeta, \tau) = & -\frac{1}{\mu^I} \left(\frac{dr^I(\tau)}{d\tau} \right) \zeta \\ & \times \left[1 - \left(K_{\text{eq}} \frac{\mu^I}{\mu^{II}} - 1 \right) \exp(v^I \zeta) \right] \\ & + \frac{l^I(\tau)}{v^I} \exp(v^I \zeta) + k^I(\tau) \end{aligned} \quad (73)$$

$$c_1^{II,\text{in}}(\zeta, \tau) = -\frac{1}{\mu^{II}} \left(\frac{dr^{II}(\tau)}{d\tau} \right) \zeta + k^{II}(\tau) \quad (74)$$

where $r^I(\tau)$, $r^{II}(\tau)$, $k^I(\tau)$, $k^{II}(\tau)$, $l^I(\tau)$ are as yet unknown functions of time τ , and $v^I = \mu^I/\phi^I$. It is worth noting that to the right of the interface there is no exponential dependence of concentration on ζ because it would increase the concentration without bound as one leaves the boundary layer.

4.3. Matching of inner and outer solutions

The perturbation analysis is completed by matching the outer and inner solutions to the left and right of the interface. Thus, as $\zeta \rightarrow \pm \infty$, $\xi \rightarrow \xi_f$,

$$c_0^{I,\text{in}} + \varepsilon c_1^{I,\text{in}} + \dots \rightarrow c_0^{I,\text{out}} + \varepsilon c_1^{I,\text{out}} + \dots \quad (75)$$

In the left region, the inner expansion through first order, $c_0^{I,\text{in}} + \varepsilon c_1^{I,\text{in}}$, grows linearly with ζ asymptotically as $\zeta \rightarrow -\infty$:

$$c_0^{I,\text{in}} + \varepsilon c_1^{I,\text{in}} \sim r^I(\tau) + \varepsilon \left[-\left(\frac{1}{\mu^I} \right) \left(\frac{dr^I(\tau)}{d\tau} \right) \zeta + k^I(\tau) \right]. \quad (76)$$

The behavior is reproduced by the outer solution, $c_0^{I,\text{out}} + \varepsilon c_1^{I,\text{out}}$, as can be seen from the Taylor expansion valid near $\xi = \xi_f$,

$$\begin{aligned} c_0^{I,\text{out}} + \varepsilon c_1^{I,\text{out}} \sim & c_0^{I,\text{out}}(\xi_f, \tau) \\ & + \left(\frac{\partial c_0^{I,\text{out}}}{\partial \xi} \right)_{\xi_f} (\xi - \xi_f) + \varepsilon c_1^{I,\text{out}}(\xi_f, \tau). \end{aligned} \quad (77)$$

Noting that $\zeta = (\xi - \xi_f)/\varepsilon$, eqs (76) and (77) are consistent if and only if

$$r^I(\tau) = c_0^{I,\text{out}}(\xi_f, \tau) \quad (78)$$

$$\frac{dr^I(\tau)}{d\tau} = -\mu^I \left(\frac{\partial c_0^{I,\text{out}}}{\partial \xi} \right)_{\xi_f} \quad (79)$$

$$k^I(\tau) = c_1^{I,\text{out}}(\xi_f, \tau). \quad (80)$$

The above equations determine the inner solution for the concentration profile to the left in terms of the corresponding outer solution. Matching of the inner and outer solutions to the right of the interface proceeds similarly but more simply owing to the absence of the exponential term. Thus, we arrive at the inner solutions

$$c_0^{I,\text{in}}(\zeta, \tau) = c_0^{I,\text{out}}(\xi_f, \tau) \left[1 + \left(K_{\text{eq}} \frac{\mu^I}{\mu^{II}} - 1 \right) \exp(v^I \zeta) \right] \quad (81)$$

$$c_0^{II,\text{in}}(\zeta, \tau) = c_0^{II,\text{out}}(\xi_f, \tau) \quad (82)$$

$$\begin{aligned} c_1^{I,\text{in}}(\zeta, \tau) = & \left[\frac{\partial c_0^{I,\text{out}}}{\partial \xi} \right]_{\xi_f} \zeta \left[1 - \left(K_{\text{eq}} \frac{\mu^I}{\mu^{II}} - 1 \right) \exp(v^I \zeta) \right] \\ & - \left[\frac{\partial c_0^{I,\text{out}}}{\partial \xi} \right]_{\xi_f} \frac{1}{v^I} \left[1 - \left(K_{\text{eq}} \frac{\mu^I}{\mu^{II}} - 1 \right) \right] \\ & \times [1 - \exp(v^I \zeta)] + \exp(v^I \zeta) [K_{\text{eq}} c_1^{II,\text{out}}(\xi_f, \tau) \\ & - c_1^{I,\text{out}}(\xi_f, \tau)] + c_1^{I,\text{out}}(\xi_f, \tau) \end{aligned} \quad (83)$$

$$c_1^{II,\text{in}}(\zeta, \tau) = \left[\frac{\partial c_0^{II,\text{out}}}{\partial \xi} \right]_{\xi_f} \zeta + c_1^{II,\text{out}}(\xi_f, \tau). \quad (84)$$

Substitution of this form into eqs (69) and (70) implies that the concentration profiles $c^{I,\text{out}}$ and $c^{II,\text{out}}$ are related as follows:

$$c_0^{II,\text{out}}(\xi_f, \tau) = \frac{\mu^I}{\mu^{II}} c_0^{I,\text{out}}(\xi_f, \tau) \quad (85)$$

$$\begin{aligned} -\phi^I \left(\frac{\partial c_0^{I,\text{out}}}{\partial \xi} \right)_{\xi_f} + \phi^I \left(K_{\text{eq}} \frac{\mu^I}{\mu^{II}} - 1 \right) \left(\frac{\partial c_0^{I,\text{out}}}{\partial \xi} \right)_{\xi_f} \\ + \mu^I c_1^{I,\text{out}}(\xi_f, \tau) = -\phi^{II} \left(\frac{\partial c_0^{II,\text{out}}}{\partial \xi} \right)_{\xi_f} \\ + \mu^{II} K_{\text{eq}} c_1^{II,\text{out}}(\xi_f, \tau). \end{aligned} \quad (86)$$

These two equations conveniently express the consequences of near-interface dynamics as interfacial conditions that can be imposed in connection with eqs (59) and (60) in determining the behavior of the macroscopically observable (outer) concentration field $c^{i,\text{out}}$. Equation (85) is analogous to the *jump mass balance* for an interface for purely convective (fluid mechanical) flow as discussed e.g. by Slattery (1981). Equation (86) gives the first-order correction to the mass balance across an interface in the presence of diffusional effects. We discuss its significance in Section 6.

4.4. Concentration profiles

Figure 2 illustrates the determination of the solute concentration from eqs (59)–(61), (85), (86) by the

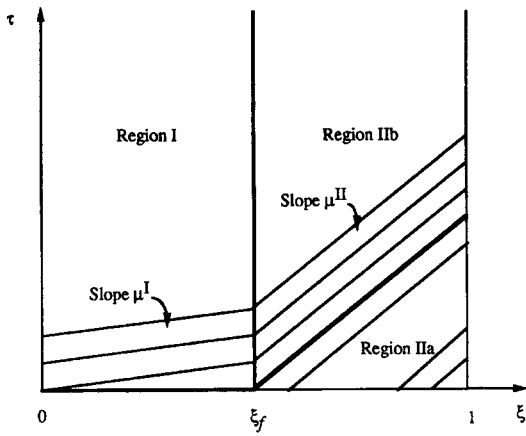


Fig. 2. Diagram of phase space for evaluating the perturbation solutions. In regions I and IIa, there is convective propagation and diffusional deformation of the initial concentration distribution along the characteristics. Near-interface dynamics comes into play in region IIb.

method of characteristics in the (ξ, τ) plane. In regions I and IIa to the left and right of the interface, the initial distributions propagate along the characteristics corresponding to the respective convective velocities v^I and v^{II} . In region IIb, the boundary layer dynamics causes the concentration propagated within region I to undergo a sudden change on passing through the interface. This change is given by eqs (85) and (86), and subsequent propagation of the concentration profile follows the characteristics in region II, viz., with a velocity v^{II} . Thus, the concentration is determined through the entire phase space. The preceding descriptive statements can be made concrete in mathematical terms. Propagation and deformation of the initial concentration distribution along the characteristics in regions I and IIa is described by the general solution of eqs (59) and (60) subject to the initial condition (61), (62) and is given by

$$\left. \begin{aligned} c_0^{I, \text{out}}(\xi, \tau) &= f_0^I(\xi - \mu^I \tau) \\ c_1^{I, \text{out}}(\xi, \tau) &= \phi^I \tau f_0^{I'}(\xi - \mu^I \tau) + f_1^I(\xi - \mu^I \tau) \end{aligned} \right] \text{region I} \quad (87)$$

$$\left. \begin{aligned} c_0^{II, \text{out}}(\xi, \tau) &= f_0^{II}(\xi - \mu^{II} \tau) \\ c_1^{II, \text{out}}(\xi, \tau) &= \phi^{II} \tau f_0^{II'}(\xi - \mu^{II} \tau) + f_1^{II}(\xi - \mu^{II} \tau) \end{aligned} \right] \text{region IIa} \quad (88)$$

where double dots denote the second derivative with respect to its argument. The concentration distribution in region I undergoes alteration due to interfacial dynamics in region IIb and this alteration is described by the equations

$$\left. \begin{aligned} c_0^{II, \text{out}}(\xi, \tau) &= \mathcal{F}_0^{II}(\xi, \tau) \\ c_1^{II, \text{out}}(\xi, \tau) &= \phi^{II} \tau (\mathcal{F}_0^{II})''(\xi, \tau) + \mathcal{F}_1^{II}(\xi, \tau) \end{aligned} \right] \text{region IIb} \quad (89)$$

where

$$\mathcal{F}_0^{II}(\xi, \tau) = \frac{\mu^I}{\mu^{II}} f_0^I(\eta) \quad (90)$$

$$\begin{aligned} \mathcal{F}_1^{II}(\xi, \tau) &= \left\{ \frac{1}{K_{\text{eq}}} \frac{\mu^I}{\mu^{II}} \left[\phi^I \tau - \left(K_{\text{eq}} \phi^{II} \tau \left(\frac{\mu^I}{\mu^{II}} \right)^2 \right) \right] f_0^{II'}(\eta) \right\} \\ &+ \frac{1}{K_{\text{eq}}} \left\{ \left[\phi^I \left(K_{\text{eq}} \frac{\mu^I}{\mu^{II}} - 1 \right) \right. \right. \\ &\left. \left. + \phi^{II} \left[\left(\frac{\mu^I}{\mu^{II}} \right)^2 \right] - \phi^I \right] f_0^I(\eta) \right\} \end{aligned} \quad (91)$$

$$\eta = \xi_f - \mu^I \left[\tau - \left(\frac{\xi - \xi_f}{\mu^{II}} \right) \right]. \quad (92)$$

The single dot denotes the first derivative with respect to its argument and the double primes represent the second derivative with respect to ξ . Equations (87)–(92) describe the outer solution to problem 1 over the entire phase space. The inner solution is obtained by substitution of the appropriate form of the outer solution into eqs (81)–(84). The complete concentration profile is obtained by evaluating the composite solution

$$c^i(\xi, \tau) = c^{i, \text{out}}(\xi, \tau) + c^{i, \text{in}}(\xi, \tau) - c^{i, \text{match}}(\xi, \tau) \quad (93)$$

where $c^{i, \text{match}}$ describes the limiting behavior of the concentration distribution in the transition from the inner to the outer region and is given by

$$\begin{aligned} c^{i, \text{match}}(\xi, \tau) &= \lim_{\xi \rightarrow \xi_f} c^{i, \text{out}}(\xi, \tau) \\ &= c_0^{i, \text{out}}(\xi_f, \tau) + \left(\frac{\partial c_0^{i, \text{out}}}{\partial \xi} \right)_{\xi_f} (\xi - \xi_f) \\ &+ \varepsilon c_1^{i, \text{out}}(\xi_f, \tau). \end{aligned} \quad (94)$$

Remark: (1) We note for completeness in regions I and IIa the outer solution to all order in ε may be written as

$$\begin{aligned} c^{i, \text{out}}(\xi, \tau) &= f_0^i(\xi - \mu^i \tau) + \varepsilon \phi^i \tau f_0^{i'}(\xi - \mu^i \tau) \\ &+ \varepsilon^2 \frac{(\phi^i)^2 \tau^2}{2} (f_0^i)^{iv}(\xi - \mu^i \tau) + \dots \\ &= f_0^i(\xi - \mu^i \tau) + \sum_{n=1}^{\infty} \varepsilon^n \sum_{m=0}^n \frac{(\phi^i)^m \tau^m}{m!} \\ &\times (f_{n-m}^i)^{2m}(\xi - \mu^i \tau) \end{aligned} \quad (96)$$

where $(f_{n-m}^i)^{2m}$ denotes the $2m$ th derivative of f_{n-m}^i with respect to its argument.

(2) Asymptotic analysis in the limit of large Péclet numbers reduces the governing equations to a set of first-order equations. The concentration profiles for all times $\tau > 0$ were determined solely from the initial distribution. Therefore, the solutions are expected to

violate the boundary conditions given by eqs (2) and (4) at $x = 0$ and $x = L$, respectively. Due to the form of the initial distribution used in our calculations, the error in concentration values at the boundaries is small. In particular, the initial distribution used has effectively tailed off to zero value and zero slope at $x = 0$ and $x = L$. In reality, boundary layers would form at the entrance and exit of the column to adjust the values of the concentration to satisfy the boundary conditions. The boundary layer would produce only small local changes in the concentration which are not essential to the solute transport and are not considered further.

5. RESULTS

Figure 3 shows the results for problems 1 and 2 for two different values of the Péclet number Pe for the case when the right-hand domain is less permeable to the solute. The interface is located at $\xi_f = 0.5$. For the purpose of illustration, we consider the case of pure electrophoretic migration, i.e. without fluid flow. We also assume that the solute is present in dilute quantities and does not contribute to the current. The convective velocity, v^i , is thus proportional to the diffusion coefficient, D^i , in the respective region. The effect of the change in transport properties across the interface has been reported in terms of the ratio of velocities $\delta = v^{II}/v^I (=D^{II}/D^I)$. We have restricted the discussion to the case where the equilibrium constant

(K_{eq}) is unity. The assumption of $\delta \neq 1$ and $K_{eq} = 1$ implies the use of a medium that offers an appreciable change in tortuosity but negligible change in the porosity across the two domains. However, both the analytical method and the perturbation analysis are valid even when the above-mentioned restrictions on δ and K_{eq} are relaxed. We further assume that terms of higher order in ε for the initial concentration distribution (f_n^i , $n > 0$) in problem 1 are identically zero. In problems 1 and 2, we see that the boundary layer thickness scales with $1/Pe$. Figures 4–6 compare the exact solutions with the perturbation analysis truncated to zeroth or first-order for three ratios of the velocities on either side of the interface. For $Pe = 50$, truncation at zeroth order reproduced qualitative features, whereas addition of the first-order term gave poor results. This is because $\varepsilon = 1/Pe$ is not small enough in this case. For $Pe = 100$, addition of the first-order term results in a slight improvement in agreement with exact results; for $Pe = 200$ addition of the first-order term produced a definite improvement. This is consistent with the general fact that the optimal asymptotic approximation includes more and more terms as the small parameter (here $\varepsilon = 1/Pe$) $\rightarrow 0$. As the value of Pe increases the results of

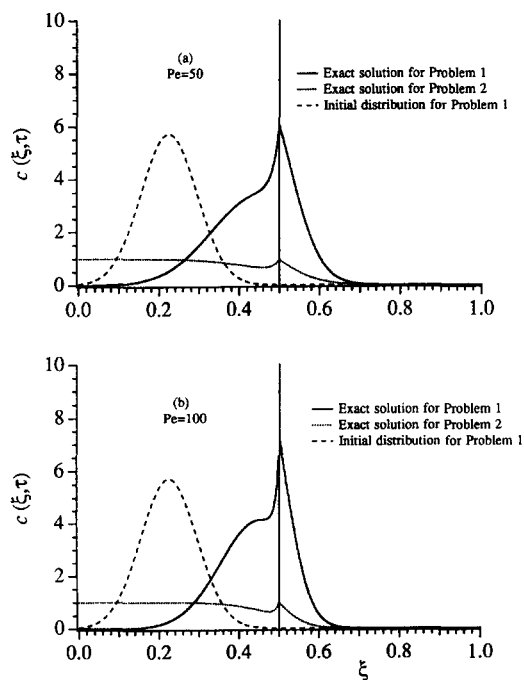


Fig. 3. Analytical solutions to problems 1 and 2 for $\delta = 0.5$. In problem 1, the initial concentration is a Gaussian distribution while in problem 2, the input concentration c_{inp} is 1. The dimensionless time τ is 0.170 and 0.375 for problems 1 and 2, respectively.

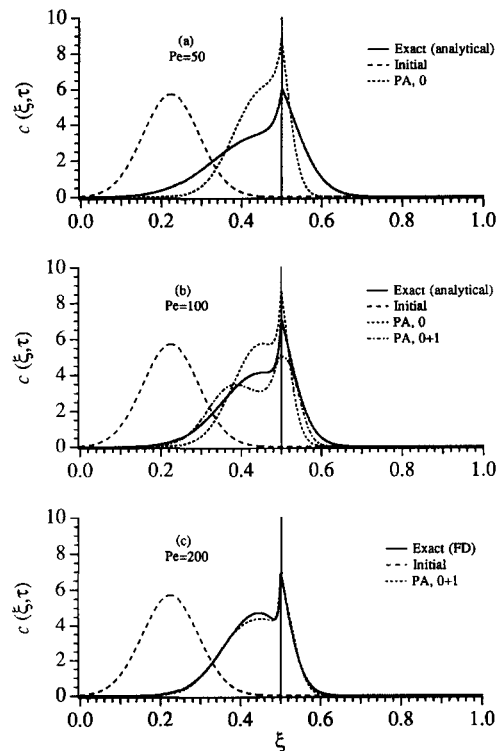


Fig. 4. Comparison of exact solution of problem 1 with the perturbation approximation (PA) at time $\tau = 0.170$ for $\delta = 0.5$ and different values of Pe . The perturbation solution in (a) has been truncated to zeroth order. Both zeroth- and first-order solutions are illustrated separately in (b). Perturbation solution in (c) is the sum of zeroth- and first-order solution.

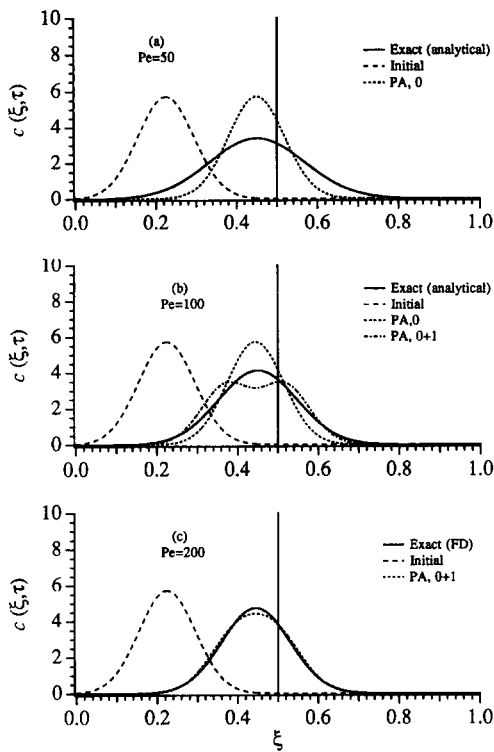


Fig. 5. Comparison of exact solution of problem 1 with the perturbation approximation at time $\tau = 0.225$ for $\delta = 1$ (no interface) and different values of Pe . The perturbation solution in (a) has been truncated to zeroth order. Both zeroth- and first-order solutions are illustrated separately in (b). Perturbation solution in (c) is the sum of zeroth- and first-order solution.

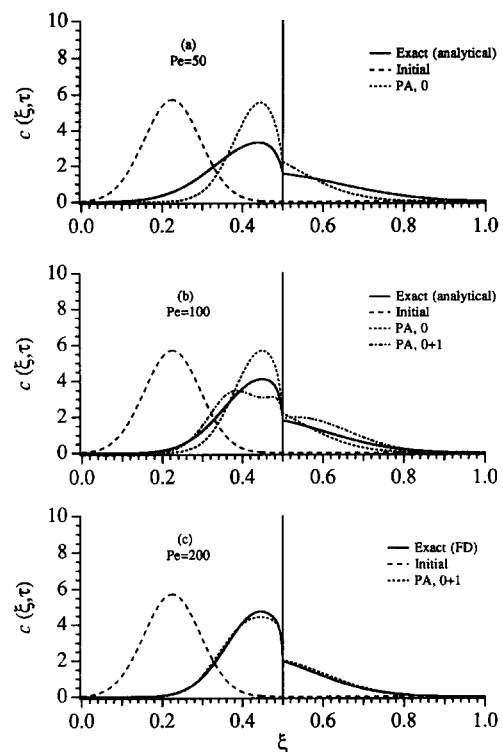


Fig. 6. Comparison of exact solution of problem 1 with the perturbation approximation at time $\tau = 0.675$ for $\delta = 2$ and different values of Pe . The perturbation solution in (a) has been truncated to zeroth order. Both zeroth- and first-order solutions are illustrated separately in (b). Perturbation solution in (c) is the sum of zeroth- and first-order solution.

perturbation analysis are expected to coincide with those of the exact solution. However, the analytical solution involving separation of variables cannot be implemented for $Pe > 100$ because it contains exponentials of Pe resulting in large roundoff errors. Hence, for Pe exceeding 100, the ‘exact’ solution was obtained using the finite-difference scheme QUICKEST (Leonard, 1979). This scheme avoids the stability problems of central differencing and reduces the inaccuracies of numerical diffusion associated with upstream differencing. Boundary layer results seem to be in very good quantitative agreement with exact results for $Pe = 200$. Perturbation analysis for the case of continuous input (problem 2) could also be performed. Owing to Danckwerts’ boundary condition, the concentration distribution is essentially discontinuous at the inlet. On performing boundary layer analysis, it is seen that the outer solution for this case is also given in terms of eq. (96) with $f_0^l(\xi - \mu^l\tau) = c_{inp}H[-(\xi - \mu^l\tau)]$ and $f_n^l(\xi - \mu^l\tau) = 0, n > 0$, where H is the Heaviside function. Thus, the outer solution is given in terms of a discontinuous function and its derivatives. Hence, results of perturbation analysis for this problem have not been presented.

6. DISCUSSION

As the results indicate, there exists a region immediately to the left of the interface which is governed by markedly different dynamics compared to the rest of the column. Here in a thin layer diffusional effects are not negligible, and the concentration in this layer decays exponentially. However, no such layer exists to the right of the interface. This can be inferred from the result that the inner solution to the right is merely the Taylor series expansion of the value of the outer solution at the interface. The boundary layer approach is accurate quantitatively for values of $Pe > 100$. For larger Pe , the analytical solution cannot be evaluated due to large roundoff errors. Finite-difference schemes, on the other hand, are capable of giving accurate results for arbitrarily large Pe 's. To ensure accuracy in the region close to the interface (modeled as a sigmoidal variation over 4 nodes), the mesh size (Δx) was set to at least a tenth of the thickness of the boundary layer. Stability of the numerical scheme for this small mesh size requires the use of a very small time step. The consequence was extremely large computational times: a 2000 node per column-length mesh required a dimensionless time step as small as 3.75×10^{-8} and resulted in 181 h of CPU time per unit simulated time τ on a Silicon

Graphics Indigo machine with the R4000 processor. The perturbation analysis achieved comparable accuracy in less than 60 s per unit simulated time τ .

The numerical calculations in Fig. 4 show a pronounced sharp peak immediately upstream of the interface. Physically, this feature of the concentration profiles represents a local accumulation of solute arising from the fact that region II is less conducive to solute transport than region I. Similarly, Fig. 6 illustrates a drop in the concentration level upstream of the interface which can be attributed to the fast depletion of solute content owing to a higher downstream velocity. This qualitative statement is made precise by the asymptotic analysis, which furnishes a quantitative description of the observed behavior and establishes the magnitudes of the peak width and height. Figures 4–6 reveal that the domain of validity of the perturbation approach does not seem to be affected by the ratio of transport properties.

In addition to facilitating the calculation of the concentration in region IIb, eqs (85) and (86) have an interesting physical interpretation. At lowest order, the solute outer flux is purely convective, and eq. (85) states that the limiting value of the convective fluxes must match at the interface lest there be local accumulation of solute. The situation is more interesting at first order. The first-order outer fluxes on the left and right sides now have both a convection contribution from c_1^i and a diffusional contribution from c_0^i , and they *do not* match, i.e. the interface appears as a source or sink of solute on a macroscopic scale. The reason is that as the zeroth-order inner concentration embodied in $c_0^{i,\text{in}}$ and $c_0^{ii,\text{in}}$ evolves, it encompasses an amount of solute that changes with time. The amount is of order ε because $c_0^{i,\text{in}}$ is of order unity and the boundary layer has thickness of order ε . Any local accumulation of solute must then be supplied from the outer region via a flux discontinuity in the outer region. More specifically, if $\mathcal{J}^{i,\text{out}}$ denotes the mass flux based on the outer solutions alone,

$$\begin{aligned}\mathcal{J}^{i,\text{out}} &= -\varepsilon\phi^i\frac{\partial c^{i,\text{out}}}{\partial \xi} + \mu^i c^{i,\text{out}} \\ &= \mu^i c_0^{i,\text{out}} + \varepsilon(-\phi^i\frac{\partial c_0^{i,\text{out}}}{\partial \xi} + \mu^i c_1^{i,\text{out}}) + \dots \\ &= \mathcal{J}_0^{i,\text{out}} + \varepsilon\mathcal{J}_1^{i,\text{out}} + \dots\end{aligned}\quad (97)$$

Let $\mathcal{J}_{0,f}^{i,\text{out}}$ and $\mathcal{J}_{1,f}^{i,\text{out}}$ denote the zeroth- and first-order outer fluxes at the interface. Then

$$\mathcal{J}_{0,f}^{ii,\text{out}} - \mathcal{J}_{0,f}^{i,\text{out}} = \mu^{ii} c_0^{ii,\text{out}}(\xi_f, \tau) - \mu^i c_0^{i,\text{out}}(\xi_f, \tau). \quad (98)$$

From eq. (85), the right-hand side of the above equation is 0:

$$\begin{aligned}\mathcal{J}_{1,f}^{ii,\text{out}} - \mathcal{J}_{1,f}^{i,\text{out}} &= -\phi^{ii}\left(\frac{\partial c_0^{ii,\text{out}}}{\partial \xi}\right)_{\xi_f} + \mu^{ii} c_1^{ii,\text{out}}(\xi_f, \tau) \\ &\quad + \phi^i\left(\frac{\partial c_0^{i,\text{out}}}{\partial \xi}\right)_{\xi_f} - \mu^i c_1^{i,\text{out}}(\xi_f, \tau) \\ &= \phi^i\left(\frac{\mu^i}{\mu^{ii}} - 1\right)\hat{f}_0(\xi_f - \mu^i\tau).\end{aligned}\quad (99)$$

The last equality in eq. (99) comes about by virtue of eq. (85) and eq. (86) for $K_{\text{eq}} = 1$. It can be verified that the right-hand side of the above equation is precisely the rate of change of the interfacial excess solute content

$$\frac{\partial}{\partial \tau} \left[\int_{-\infty}^{\infty} (c_0^{i,\text{out}} - c_0^{i,\text{in}}) d\xi \right]. \quad (100)$$

Thus, dynamical processes in the boundary layer imbues the interface (which appears infinitesimally thin from a macroscopic viewpoint) with an effective source/sink character.

7. CONCLUSION

A novel analytical approach to solving transport problems in discontinuous media has been presented (Section 3). This approach is, in principle, valid for any Pe . In practice, the approach breaks down for $Pe > 100$ due to large round off errors. Hence, it cannot be implemented for accurate prediction of the dynamics of the region near the interface where diffusional resistance cannot be neglected. Finite-difference techniques can yield accurate results for arbitrarily large Pe in a continuous medium. For a medium with a region of infinite gradients in transport properties, these methods tend to be unstable unless the region of discontinuity is approximated with a sharp but continuous transition. For high Pe , this implies very fine meshes, very small time increments and consequently very large computational times. The large- Pe perturbation approach is very suitable for such cases. It is seen to yield accurate results with almost 10^4 -fold reduction in computation time.

Acknowledgements—The authors gratefully acknowledge support of this research by the National Science Foundation through the Presidential Young Investigator Program (D.A.K.) and National Young Investigator Program (J.M.N. and S.L.D.), as well as National American Heart Association Grant-in-Aid 93-8670 (S.L.D.). Calculations were performed on computing equipment obtained with support from the National Science Foundation, Grant no. CTS-9212682.

NOTATION

a	time constant, 1/s
A	Fourier coefficient, mol/m ³
b	time constant, 1/s
c	concentration of solute, mol/m ³
D	diffusion coefficient, m ² /s
E	electric field, V/m
f	actual initial concentration distribution, mol/m ³
F	Faraday's constant, 96,500 C/mol
\mathcal{F}	downstream concentration distribution, mol/m ³
g	modified initial concentration distribution, mol/m ³
G	kernel in eq. (32), m/s
h	constant, 1/m
I	integral term, m
k	parameter in eq. (73), mol/m ³

K_{eq}	equilibrium constant, dimensionless
l	parameter in eq. (73), mol/m ³
L	length of column, m
L_f	location of interface from column entrance, m
p	Fourier coefficient, dimensionless
P	modified Boltzmann distribution in eq. (19), dimensionless
Pe	mean Péclet number, dimensionless
Q	flux term in eq. (32), mol/m s
r	parameter in eq. (73), mol/m ³
R	universal gas constant, J/(mol K)
s	modified concentration of solute, mol/m ³
S	components of kernel G, m/s
t	time, s
T	temperature, K
v	velocity, m/s
W	inhomogeneous term in eq. (18), mol/m ³ s
x	lab-fixed spatial coordinate, m
X	basis (eigen) function, dimensionless
z	valency of the solute

Greek letters

α	eigenvalue, 1/m
β	spatial coordinate, m
γ	parameter in eq. (A7), 1/m
δ	ratio of downstream to upstream velocity, dimensionless
ε	inverse mean Péclet number
ζ	stretched spatial coordinate, dimensionless
η	parameter defined in eq. (92), dimensionless
λ	parameter in eq. (A7), 1/m
μ	dimensionless velocity
ν	ratio of dimensionless velocity to dimensionless diffusion coefficient
ξ	dimensionless lab-fixed spatial coordinate
ρ	modified concentration in problem 2, mol/m ³
σ	time in Appendix B, s
τ	dimensionless time
ϕ	dimensionless diffusion coefficient

Superscripts

–	average between two domains
·	derivative w.r.t. argument
'	derivative w.r.t. ξ
i	upstream or downstream domain
in	inner region
I	upstream domain
II	downstream domain
match	transition region between inner and outer region
out	outer region

Subscripts

f	interface
inp	input
n	index of Fourier expansion term

REFERENCES

- Arce, P. and Locke, B. R., 1994, Transport and reaction: an integral equation approach: mathematical formulation and computational approaches, In *Trends in Chemical Engineering*, Vol. 2, pp. 89–158. Council of Scientific Research Integration, India.
- Brenner, H., 1962, The diffusion model of longitudinal mixing in beds of finite length. Numerical values. *Chem. Engng Sci.* **44**, 827–840.
- Carrier, G. F. and Pearson, C. E., 1976, *Partial Differential Equations—Theory and Technique*. Academic Press, New York, U.S.A.
- Clark, W. M., 1992, Electrophoresis-enhanced extractive separation. *Chemtech* **22**, 425–429.
- Dankwerts, P. V., 1953, Continuous flow systems. Distribution of residence times. *Chem. Engng Sci.* **2**, 1–18.
- de Gennes, P. G. and Prost, J., 1993, *The Physics of Liquid Crystals*, 2nd Edn. Clarendon Press, Oxford, U.K.
- Grimshaw, P. E., Grodzinsky, A. J., Yarmush, M. L. and Yarmush, D. M., 1989, Dynamic membranes for protein transport: chemical and electrical control. *Chem. Engng Sci.* **44**, 827–840.
- Hladky, S. B., 1987, The effect of diffusion and convection on the rate of transfer of solutes across an interface. *Eur. Biophys. J.* **15**, 251–255.
- Ince, E. L., 1956, *Ordinary Differential Equations*, p. 63. Dover, New York, U.S.A.
- Kim, S. and Karrila, S. J., 1991, *Microhydrodynamics: Principles and Selected Applications*, Butterworth-Heinemann, Boston, U.S.A. and U.K.
- Kreyszig, E., 1993, *Advanced Engineering Mathematics*, 7th Edn, pp. 241–246. Wiley, New York, U.S.A.
- Leonard, B. P., 1979, A stable and accurate convective modelling procedure based on quadratic upstream interpolation. *Comput. Meth. Appl. Mech. Engng* **19**, 59–98.
- Levine, M. L. and Bier, M., 1990, Electrophoretic transport of solutes in aqueous two-phase systems. *Electrophoresis* **11**, 605–611.
- Levine, M. L., Cabezas, H. and Bier, M., 1992, Transport of solutes across aqueous phase interfaces by electrophoresis. Mathematical modeling. *J. Chromatogr.* **607**, 113–118.
- Locke, B. R. and Arce, P., 1993, Applications of self-adjoint operators to electrophoretic transport, enzyme reactions, and microwave heating problems in composite media—I. General formulation. *Chem. Engng Sci.* **48**, 1675–1686.
- Locke, B. R., Arce, P. and Park, Y., 1993, Applications of self-adjoint operators to electrophoretic transport, enzyme reactions, and microwave heating problems in composite media—II. Electrophoretic transport in layered membranes. *Chem. Engng Sci.* **48**, 4007–4022.
- Ly, Y. and Cheng, Y.-L., 1993, Electrically-modulated variable permeability liquid crystalline polymeric membrane. *J. Membrane Sci.* **77**, 99–112.
- Novy, R. A., Davis, H. T. and Scriven, L. E., 1990, Upstream and downstream boundary conditions for continuous-flow systems. *Chem. Engng Sci.* **45**, 1515–1524.
- Raj, C. B. C., 1994, Protein purification by counteracting chromatographic electrophoresis: quantitative focusing limits and protein selection at the interface. *J. Biochem. Biophys. Methods* **28**, 161–172.
- Ramkrishna, D. and Amundson, N. R., 1974, Transport in composite materials: reduction to a self adjoint formalism. *Chem. Engng Sci.* **29**, 1457–1464.
- Slattery, J. C., 1981, *Momentum, Energy, and Mass Transfer in Continua*, pp. 22–25. McGraw-Hill Book Co., New York, U.S.A.
- Weinberger, H. F., 1965a, *A First Course in Partial Differential Equations*, Chap. IV. Wiley, New York, U.S.A.
- Weinberger, H. F., 1965b, *A First Course in Partial Differential Equations*, Chap. VII. Wiley, New York, U.S.A.

APPENDIX A

The sums $G^l(t; \tau)$ and $G^{ll}(t; \tau)$ in eqs (37) and (38) were found to diverge at $\tau = t$. This is because as $n \rightarrow \infty$, the terms

$\alpha_n^i p_n^i$ and $\alpha_n^i p_n^{\text{II}}$ do not vanish but rather approach constant values of $(-2/L_f)$ and $[2/(L-L_f)]$, respectively. Based on physical considerations, the interfacial concentrations on either side must remain finite. This implies that although the sums $G^i(t; \tau)$ and $G^{\text{II}}(t; \tau)$ diverge at $\tau = t$, the integrals containing these sums remain finite. In order to evaluate these integrals, we expand the coefficients α_n^i , $(\alpha_n^i)^2$ and $\alpha_n^i p_n^i$ in orders of $1/n$. We then add and subtract the leading terms of these terms from the series $G^i(t; \tau)$ and $G^{\text{II}}(t; \tau)$. In doing so, we express the singularity in each of these series in terms of another singular series whose asymptotic behavior in the region of divergence is known. The leading terms of the above coefficients are given by

$$\alpha_n^i = \left(n - \frac{1}{2}\right) \frac{\pi}{\lambda^i} + \left(\frac{h^i}{\pi}\right) \frac{1}{n} + \left(\frac{h^i}{2\pi}\right) \frac{1}{n^2} + O\left(\frac{1}{n^3}\right) \quad (\text{A1})$$

$$(\alpha_n^i)^2 = \left[\left(n - \frac{1}{2}\right) \frac{\pi}{\lambda^i}\right]^2 + \left(\frac{2h^i}{L_f}\right) + \frac{0}{n} - \left[\left(\frac{h^i \lambda^i}{\pi}\right)^2 + \frac{5}{3} \left(\frac{h^i \lambda^i}{\pi}\right)^3\right] \frac{1}{n^2} + O\left(\frac{1}{n^3}\right) \quad (\text{A2})$$

$$\alpha_n^i p_n^i = \frac{1}{\gamma^i} \left[-2 + \frac{0}{n} + \frac{2(h^i \lambda^i)(h^i \lambda^i - 1)}{\pi^2} \frac{1}{n^2} + O\left(\frac{1}{n^3}\right)\right] \quad (\text{A3})$$

where $\gamma^i, \lambda^i = L_f$ for $i = \text{I}$ and $\gamma^i = -(L - L_f)$, $\lambda^i = L - L_f$ for $i = \text{II}$. The kernels $G^i(t; \tau)$ are then given in terms of three sums,

$$G^i(t; \tau) = S_1^i(t; \tau) + S_2^i(t; \tau) + S_3^i(t; \tau) \quad (\text{A4})$$

where

$$S_1^i(t; \tau) = D^i \exp[-a^i(t - \tau)] \sum_{n=1}^{\infty} \left(\alpha_n^i p_n^i + \frac{2}{\gamma^i}\right) \times \exp[-(\alpha_n^i)^2 D^i(t - \tau)] \quad (\text{A5})$$

$$S_2^i(t; \tau) = \frac{-2}{\gamma^i} D^i \exp[-a^i(t - \tau)] \times \exp\left[\frac{-2h^i}{\lambda^i} D^i(t - \tau)\right] \sum_{n=1}^{\infty} \left\{ \exp\left[-\left(\alpha_n^i\right)^2\right] - \left[\left(n - \frac{1}{2}\right) \frac{\pi}{\lambda^i}\right]^2 - \left(\frac{-2h^i}{\lambda^i}\right) \right\} \times D^i(t - \tau) - 1 \quad (\text{A6})$$

$$S_3^i(t; \tau) = \frac{-2}{\gamma^i} D^i \exp[-a^i D^i(t - \tau)] \times \exp\left[\frac{-2h^i}{\lambda^i} D^i(t - \tau)\right] \sum_{n=1}^{\infty} \left\{ -\left[\left(n - \frac{1}{2}\right) \frac{\pi}{\lambda^i}\right]^2 D^i(t - \tau) \right\} \quad (\text{A7})$$

Here $S_1^i(t; \tau)$ and $S_2^i(t; \tau)$ contain pre-exponential terms which decay as $1/n^2$ and hence these sums are uniformly convergent even for $\tau = t$. For convenience, let $S_{12}^i(t; \tau)$ denote $S_1^i(t; \tau) + S_2^i(t; \tau)$. The sum $S_3^i(t; \tau)$, on the other hand, is divergent as $\tau \rightarrow t$. To identify its asymptotic behavior in the region of divergence, we consider the series $S_y = \sum_{n=1}^{\infty} y^{(n-1/2)^2}$ for $0 \leq y < 1$. From Fig. A1 it is seen that

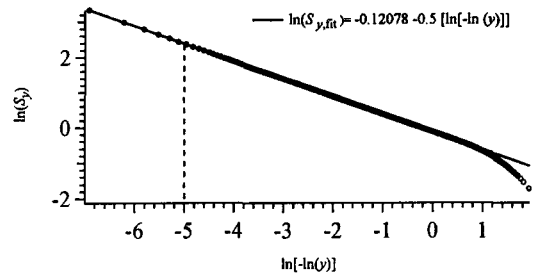


Fig. A1. The series S_y in the domain $0 \leq y < 1$. The open circles represent the actual value of S_y . The solid line represents the asymptotic behavior as $y \rightarrow 1$ obtained by curve fitting.

$S_y \cong (\pi/\sqrt{2})[-\ln(y)]^{-1/2}$ for y exceeding a critical value {here taken as $\ln[-\ln(y)] = -5$ or $y = 0.993$ }. Therefore for τ exceeding a critical value τ_c , the sum $S_3^i(t; \tau)$ can be expressed in its asymptotic form as given below,

$$S_3^i(t; \tau) \cong -\sqrt{2D^i} \frac{\lambda^i}{\gamma^i \sqrt{t - \tau}} \quad (\tau > \tau_c) \quad (\text{A8})$$

where τ_c is given by

$$\exp\left[-\frac{\pi^2 D^i(t - \tau_c)}{(\lambda^i)^2}\right] = 0.993 \quad (\text{A9})$$

The sums $G^i(t; \tau)$ and $G^{\text{II}}(t; \tau)$ are now integrable as $\tau \rightarrow t$ because the sums $S_1^i(t; \tau)$ and $S_2^i(t; \tau)$ as given by the above equations contain a finite area under the curve in the interval $[0, t]$.

The integrodifferential equation (32) can now be solved in the following manner. The interval of integration $[0, t]$ is discretized into steps of width Δt chosen such that $\Delta t \ll t - \tau_c$. The integral terms are evaluated as a sum over the subintervals $[0, t - \Delta t]$ and $[t - \Delta t, t]$. The sums $G^i(t; \tau)$ and $G^{\text{II}}(t; \tau)$ remain convergent in the subinterval $0 \leq \tau \leq t - \Delta t$ due to significant contribution from their exponential decay terms. The singular behavior of $G^i(t; \tau)$ and $G^{\text{II}}(t; \tau)$ is restricted to the remainder of the interval of integration, viz., $t - \Delta t < \tau \leq t$. In this small subinterval, the two kernels are written according to eqs (A4)–(A7). On making these changes and substituting them in the integrodifferential equation we get

$$Q(t) + K_{\text{eq}} \int_0^{t-\Delta t} \frac{dc_f^{\text{II}}(\tau)}{d\tau} G^i(t; \tau) d\tau + K_{\text{eq}} \left(\frac{dc_f^{\text{II}}(\tau)}{d\tau}\right)_{\tau=t} \times \int_{t-\Delta t}^t [S_{12}^i(t; \tau) + S_3^i(t; \tau)] d\tau = \int_0^{t-\Delta t} \frac{dc_f^{\text{II}}(\tau)}{d\tau} G^{\text{II}}(t; \tau) d\tau + \left(\frac{dc_f^{\text{II}}(\tau)}{d\tau}\right)_{\tau=t} \times \int_{t-\Delta t}^t [S_{12}^{\text{II}}(t; \tau) + S_3^{\text{II}}(t; \tau)] d\tau + v^{\text{II}} c_f^{\text{II}}(t). \quad (\text{A10})$$

In writing the above equation, we have assumed that the concentration gradient does not change significantly in the small interval $[t - \Delta t, t]$ and can therefore be approximated with its value at $\tau = t$ which can then be placed outside the integral. The time derivative of the interfacial concentration is approximated with a simple upstream difference formula, viz.,

$$\frac{dc_f^{\text{II}}(\tau)}{d\tau} = \frac{c_f^{\text{II}}(\tau) - c_f^{\text{II}}(\tau - \Delta t)}{\Delta t} \quad (\text{A11})$$

On substituting this in eq. (A10), the interfacial concentration at time t may be written in terms of its value at previous instances of time as follows:

$$c_f^{\text{II}}(t) = \frac{Q(t) + (K_{\text{eq}} I_1 - I_2) - \left\{ \frac{[c_f^{\text{II}}(t - \Delta t)](K_{\text{eq}} I_1^c + I_1^s - K_{\text{eq}} I_2^c - I_2^s)}{\Delta t} \right\}}{v^{\text{II}} - \left[\frac{(K_{\text{eq}} I_1^c + I_1^s - K_{\text{eq}} I_2^c - I_2^s)}{\Delta t} \right]} \quad (\text{A12})$$

where

$$I_1 = \int_0^{t-\Delta t} \frac{c_f^{\text{II}}(\tau) - c_f^{\text{II}}(\tau - \Delta t)}{\Delta t} G^{\text{I}}(t; \tau) \, d\tau \quad (\text{A13})$$

$$I_2 = \int_0^{t-\Delta t} \frac{c_f^{\text{II}}(\tau) - c_f^{\text{II}}(\tau - \Delta t)}{\Delta t} G^{\text{II}}(t; \tau) \, d\tau \quad (\text{A14})$$

$$I_1^c = \int_0^{t-\Delta t} S_{12}^{\text{I}}(t; \tau) \, d\tau \quad (\text{A15})$$

$$I_2^c = \int_0^{t-\Delta t} S_{12}^{\text{II}}(t; \tau) \, d\tau \quad (\text{A16})$$

$$I_1^s = \int_{t-\Delta t}^t S_3^{\text{I}}(t; \tau) \, d\tau = -2 \frac{\lambda_i}{\gamma_i} \sqrt{2D^{\text{I}} \Delta t} \quad (\text{A17})$$

$$I_2^s = \int_{t-\Delta t}^t S_3^{\text{II}}(t; \tau) \, d\tau = -2 \frac{\lambda_i}{\gamma_i} \sqrt{2D^{\text{II}} \Delta t}. \quad (\text{A18})$$

The first four integrals were evaluated with the trapezoidal rule. Finally, the interfacial concentration at time t is evaluated by successive determination of its value at all intermediate steps between 0 and the required time.

For large Pe , calculating the concentration profiles from the analytical solution suffered increasingly from numerical difficulties. These problems stemmed from the need to take exponentials of numbers of $O(Pe)$ and, after some manipulation, dividing them again by numbers of equivalent magnitude. The process first resulted in simple round-off errors, then overflows. The problem is worst for concentrations away from the interface, and in fact for $Pe = 100$ we found spurious peaks in the concentrations near the end of the column; these were set to zero before presenting our results.

APPENDIX B

In this section, we describe the analysis of the limiting case of infinite Pe for the transient transport of a solute in a dynamic discontinuous medium. As before the transport properties of the solute remain constant on either side of the interface but the interface itself is allowed to migrate with an externally imposed velocity that can be a function of time. Liquid crystals (de Gennes and Prost, 1993) offer a good example of such dynamic materials and are gaining increasing importance in chemical engineering applications.

Consider the case of solute migration in a discontinuous medium with a sharp interface that can be moved with an imposed velocity $v_f(t)$ such that its location at any time t is given by $L_f(t) = L_f(0) + \int_0^t v_f(s) ds$, where $L_f(0)$ is the position of the interface at time $t = 0$. We shall restrict the analysis to conditions of negligible diffusional effects, i.e. $Pe \rightarrow \infty$. Ignoring diffusional contribution to solute transport requires that the interface velocity $v_f(t)$ be much smaller than the solute convective velocities v^{I} and v^{II} . For cases where the interface velocity lies between the values of the convective

velocities ($v^{\text{II}} < v_f(t) < v^{\text{I}}$), the solute will catch up with the plane of discontinuity and thereafter the entire solute content will move with the same velocity as that of the interface.

The change in its effective velocity from v^{I} to $v_f(t)$ can be attributed to diffusional resistance to mass transport which becomes significant whenever the solute lies within $O(Pe^{-1})$ distance from the interface. Thus, for this range of the interface velocity, the transient mass transport of the solute cannot be adequately described by the asymptotic analysis in the limit of infinite Pe .

Using the same notation as before to denote $i = \text{I, II}$ for the left and right domains, respectively, the mass balance in each domain (for $v_f(t) < v^{\text{I}}, v^{\text{II}}$) may be written as

$$\frac{\partial c^{\text{I}}}{\partial t} + v^{\text{I}} \frac{\partial c^{\text{I}}}{\partial x} = 0, \quad x < L_f(t) \quad (\text{B1})$$

$$\frac{\partial c^{\text{II}}}{\partial t} + v^{\text{II}} \frac{\partial c^{\text{II}}}{\partial x} = 0, \quad x > L_f(t). \quad (\text{B2})$$

We assume that there is an initial concentration distribution in the left domain while the right domain is empty. On contacting the interface, the concentration undergoes a sudden change owing to local dynamics as discussed in relation with eq. (85). The above initial and boundary conditions can be represented mathematically as

$$c^{\text{I}}(x, 0) = f^{\text{I}}(x) \quad (\text{B3})$$

$$c^{\text{II}}(x, 0) = 0 \quad (\text{B4})$$

$$\{v^{\text{I}} - v_f(t)\} c^{\text{I}}(L_f(t), t) = \{v^{\text{II}} - v_f(t)\} c^{\text{II}}(L_f(t), t). \quad (\text{B5})$$

We introduce the coordinates (β, σ) such that the location of the interface in this coordinate system is independent of time. The new coordinate system is defined by the transformation

$$\begin{aligned} \beta &= x - \int_0^t v_f(s) \, ds \\ &= x - L_f(t) + L_f(0) \end{aligned} \quad (\text{B6})$$

$$\sigma = t. \quad (\text{B7})$$

The conservation equations along with the initial and boundary conditions in the transformed coordinate system are given by

$$\frac{\partial c^{\text{I}}}{\partial \sigma} + v_f^{\text{I}}(\sigma) \frac{\partial c^{\text{I}}}{\partial \beta} = 0, \quad \beta < L_f(0) \quad (\text{B8})$$

$$\frac{\partial c^{\text{II}}}{\partial \sigma} + v_f^{\text{II}}(\sigma) \frac{\partial c^{\text{II}}}{\partial \beta} = 0, \quad \beta > L_f(0) \quad (\text{B9})$$

$$c^{\text{I}}(\beta, 0) = f^{\text{I}}(\beta) \quad (\text{B10})$$

$$c^{\text{II}}(\beta, 0) = 0 \quad (\text{B11})$$

$$v_f^{\text{I}}(\sigma) c^{\text{I}}(L_f(0), \sigma) = v_f^{\text{II}}(\sigma) c^{\text{II}}(L_f(0), \sigma) \quad (\text{B12})$$

where $v_r^I(\sigma) = [v^I - v_f(\sigma)]$ and $v_r^II(\sigma) = [v^{II} - v_f(\sigma)]$ denote the velocities in each domain relative to the front. The solution to this system of equations is given by the method of characteristics (Carrier and Pearson, 1976) as

$$c^I(\beta, \sigma) = f^I(\beta_1) \quad (\text{B13})$$

$$c^{II}(\beta, \sigma) = \frac{v_r^I(\sigma + \alpha)}{v_r^{II}(\sigma + \alpha)} f^I(\beta_2) \quad (\text{B14})$$

where α is the solution to

$$\int_{\sigma}^{\sigma + \alpha} v_r^{II}(s) \, ds = L_f(0) - \beta \quad (\text{B15})$$

and β_1 and β_2 are given by

$$\beta_1 = \eta - \int_0^{\sigma} v_r^I(s) \, ds \quad (\text{B16})$$

$$\beta_2 = L_f(0) - \int_0^{\sigma + \alpha} v_r^I(s) \, ds. \quad (\text{B17})$$